Published in final edited form as:
J Pharmacokinet Pharmacodyn. 2012 December ; 39(6): 711–723. doi:10.1007/s10928-012-9280-2.

Applications of minimal physiologically-based pharmacokinetic models

Yanguang Cao and
Department of Pharmaceutical Sciences, School of Pharmacy and Pharmaceutical Sciences, State University of New York at Buffalo, 404 Kapoor Hall, Buffalo, NY 14214-8033, USA

William J. Jusko
Department of Pharmaceutical Sciences, School of Pharmacy and Pharmaceutical Sciences, State University of New York at Buffalo, 404 Kapoor Hall, Buffalo, NY 14214-8033, USA

William J. Jusko: wjjusko@buffalo.edu

Abstract

Conventional mammillary models are frequently used for pharmacokinetic (PK) analysis when only blood or plasma data are available. Such models depend on the quality of the drug disposition data and have vague biological features. An alternative minimal-physiologically-based PK (minimal-PBPK) modeling approach is proposed which inherits and lumps major physiologic attributes from whole-body PBPK models. The body and model are represented as actual blood and tissue usually total body weight) volumes, fractions (f_d) of cardiac output with Fick's Law of Perfusion, tissue/blood partitioning (K_p), and systemic or intrinsic clearance. Analyzing only blood or plasma concentrations versus time, the minimal-PBPK models parsimoniously generate physiologically-relevant PK parameters which are more easily interpreted than those from mammillary models. The minimal-PBPK models were applied to four types of therapeutic agents and conditions. The models well captured the human PK profiles of 22 selected beta-lactam antibiotics allowing comparison of fitted and calculated K_p values. Adding a classical hepatic compartment with hepatic blood flow allowed joint fitting of oral and intravenous (IV) data for four hepatic elimination drugs (dihydrocodeine, verapamil, repaglinide, midazolam) providing separate estimates of hepatic intrinsic clearance, non-hepatic clearance, and pre-hepatic bioavailability. The basic model was integrated with allometric scaling principles to simultaneously describe moxifloxacin PK in five species with common K_p and f_d values. A basic model assigning clearance to the tissue compartment well characterized plasma concentrations of six monoclonal antibodies in human subjects, providing good concordance of predictions with expected tissue kinetics. The proposed minimal-PBPK modeling approach offers an alternative and more rational basis for assessing PK than compartmental models.

Keywords

PBPK; Mammillary model; Pharmacokinetics; Compartmental analysis

Correspondence to: William J. Jusko, wjjusko@buffalo.edu.

Electronic supplementary material The online version of this article (doi:10.1007/s10928-012-9280-2) contains supplementary material, which is available to authorized users.

Introduction

Physiologically-based pharmacokinetic models (PBPK) are more mechanistic than 'classical' compartmental models as they incorporate anatomical and physiological knowledge into descriptions of pharmacokinetics (PK) [1]. Building such models, however, requires measurements of drug concentrations in numerous organs and tissues. When only blood or plasma data is available, the convention is to apply noncompartmental (NCA) and/or compartmental analysis [2]. However, mammillary models represent the body as a system of compartments that usually have limited physiologic or anatomic reality. They are highly dependent on the intensity of the blood collection schedule and make no prior use of the physiology of the organism [3, 4]. An intermediate perspective between full PBPK and compartmental models would be helpful. Recirculatory models offer a somewhat more physiologically realistic approach to describe PK in which flows to tissue spaces are considered [5]. These models usually require some empirical adjustments and are not often utilized as they are difficult to implement and interpret [6, 7].

'Lumping' is a commonly employed approach to reduce the dimensionality and complexity of whole body PBPK models placing tissues that show similar kinetics together to form fewer compartments [8, 9]. Whole body PBPK models are often successfully represented by a limited number of 'lumped' compartments. A PBPK model with only four organs was previously constructed for warfarin [10]. Some organs (muscle, fat, kidney) that exhibited similar kinetics could be further lumped in this model, and the time course of serum warfarin concentrations was mainly supported by nonlinear (liver) and linear tissue distribution components.

The concept of 'hybrid-PBPK' models has been utilized in previous studies by using plasma concentration functions with perfusion input to specific organs (mostly liver, kidney, brain, or tumor) [11–13]. This allows more detailed descriptions of drug exposures or disposition for specific tissues. Henthorn et al. [14] employed the term 'minimal' compartment model in constructing a parallel channel, lumped-parameter circulatory model for disposition of indocyanine green in dogs.

This report proposes a generalized minimal-PBPK modeling approach which represents the system as a substantially lumped PBPK model. The incorporation of physiological and anatomical knowledge into the minimal-PBPK models allows separation of system- and drug-specific parameters and permits consideration of known physicochemical and metabolic properties in determination of drug PK features (Fig. 1). Applications of the minimal-PBPK models will be shown by characterizing several types of drugs in different situations, revealing better PK insights than conventional mammillary models.

Model structures

Figure 2 shows a minimal-PBPK model with two tissue compartments. The model is described using the differential equation structure similar to PBPK models:

$$\frac{dC_P}{dt}=\frac{Input}{V_P}+f_{d1}\cdot Q_{CO}\cdot\frac{C_1}{K_{P1}\cdot V_P}+f_{d2}\cdot Q_{CO}\cdot\frac{C_2}{K_{P2}\cdot V_P}-\frac{C_P}{V_P}\cdot(f_{d1}\cdot Q_{CO}+f_{d2}\cdot Q_{CO}+CL) \quad C_P(0)=0 \quad (1)$$

$$\frac{dC_1}{dt}=\left(C_P-\frac{C_1}{K_{P1}}\right)\cdot f_{d1}\cdot Q_{CO}/V_1 \quad C_1(0)=0 \quad (2)$$

$$\frac{dC_2}{dt}=\left(C_P-\frac{C_2}{K_{P2}}\right)\cdot f_{d2}\cdot Q_{CO}/V_2 \quad C_2(0)=0 \quad (3)$$

where C_p is concentration of drug in V_p (blood or plasma volume), C_1 and C_2 are drug concentrations in tissue compartments 1 (V_1) and 2 (V_2), Q_{CO} is cardiac blood (or plasma) flow, f_{d1} and f_{d2} are fractions of Q_{CO} for V_1 and V_2, K_{p1} and K_{p2} are tissue partition coefficients, and CL is the systemic clearance.

The key features of this model are the physiological restrictions where V_p is the designated blood or plasma volume, Q_{CO} is the assigned cardiac output, and:

$$f_{d1}+f_{d2}\le 1$$
$$V_1+V_2+V_p=BW \text{ or } ECF$$
(Body weight or extracellular fluid volume).

This allows V_2 to be treated as a secondary parameter with only estimation of V_1.

The model was further extended by including the liver to describe oral dosing with hepatic first-pass as shown in Fig. 3. The modified model equations are:

$$\begin{aligned}\frac{dC_P}{dt}=&\frac{Input}{V_p}+f_{d1}\cdot(Q_{CO}-Q_{hep})\cdot\frac{C_1}{K_P\cdot V_P}\\&+f_{d2}\cdot(Q_{CO}-Q_{hep})\cdot\frac{C_2}{K_P\cdot V_P}\\&+Q_{hep}\cdot(\frac{C_{hep}}{K_P}-C_P)/V_P-C_P\cdot[f_{d1}\cdot(Q_{CO}-Q_{hep})\\&+f_{d2}\cdot(Q_{CO}-Q_{hep})+CL_{non-hep}]/V_P \quad C_P(0)=0\end{aligned} \quad (4)$$

$$\frac{dC_1}{dt}=\left(C_P-\frac{C_1}{K_P}\right)\cdot f_{d1}\cdot(Q_{CO}-Q_{hep})/V_1 \quad C_1(0)=0 \quad (5)$$

$$\frac{dC_2}{dt}=\left(C_P-\frac{C_2}{K_P}\right)\cdot f_{d2}\cdot(Q_{CO}-Q_{hep})/V_2 \quad C_2(0)=0 \quad (6)$$

$$\frac{dC_{hep}}{dt}=[F_G\cdot Dose\cdot e^{-k_a\cdot t}+Q_{hep}\cdot\left(C_P-\frac{C_{hep}}{K_P}\right)-\frac{C_{hep}}{K_{P\,intu}}]/V_{hep} \quad C_{hep}(0)=0 \quad (7)$$

where Q_{hep} is portal vein blood flow, C_{hep} is drug concentration in liver compartment (V_{hep}), CL_{intu} and $CL_{non\text{-}hep}$ are unbound hepatic intrinsic and non-hepatic clearances, and F_G and k_a are pre-hepatic bioavailability and the absorption rate constant. Other symbols represent the same parameters as in Fig. 2. The physiological restrictions of these parameters are:

$$f_{d1}+f_{d2}\le 1 \text{ and } V_1+V_2+V_p+V_{hep}=BW \text{ or } ECF$$

The extended model with a hepatic compartment (Fig. 3) can be related to clearance concepts of Rowland et al. [15] who proposed the well-stirred model:

$$CL_{hep}=\frac{Q_{hep}\cdot f_{up}\cdot CL_{intu}}{Q_{hep}+f_{up}\cdot CL_{intu}}=Q_{hep}\cdot ER \quad (8)$$

which often works well for relating hepatic clearance (CL_{hep}) to intrinsic clearance (CL_{intu}), fraction unbound in plasma (f_{up}), and extraction ratio (ER). With addition of F_G and k_a, the minimal-PBPK model can account for both oral and IV profiles. The extended model separates clearances by liver (CL_{intu}) and other tissues ($CL_{non\text{-}hep}$). Hepatic clearance (CL_{hep}) can be calculated from CL_{intu} that is estimated based upon liver free concentration where $1/K_p$ is fraction unbound in the liver when $f_{up} = 1$.

A basic model was applied to assess the PK of several monoclonal antibodies (mAb) as shown in Fig. 4. Since elimination of mAb mostly occurs in the tissue interstitial space [16], the clearance (CL_T) was assigned to the tissue compartment (Model A) and compared with model with clearance (CL_P) from plasma (Model B). The Model A equations are:

$$\frac{dC_p}{dt}=\frac{Input}{V_p}+f_d\cdot Q_{CO}\cdot\left(\frac{C_t}{K_p}-C_p\right)/V_p \quad C_p(0)=0 \quad (9)$$

$$\frac{dC_t}{dt}=f_d\cdot\frac{Q_{CO}}{V_t}\cdot\left(C_p-\frac{C_t}{K_p}\right)-\frac{C_t}{V_t}\cdot CL_T \quad C_t(0)=0 \quad (10)$$

where Q_{CO} is specifically designated as plasma cardiac output for mAb and CL_T was assumed to be relevant with total concentration of mAb in tissue. The physiological restrictions of relevant parameters are: $f_d \le 1$ and $V_t + V_p = BW$.

Data analysis

The proposed minimal-PBPK models were applied to several PK data sets that were found in the literature: beta-lactam antibiotics [17–36], hepatic elimination drugs (dihydrocodeine [37], verapamil [38], repaglinide [39], and midazolam [40]), moxifloxacin PK in five species [41], and six mAbs PK in human subjects [42–47]. Concentration–time data were obtained via computer digitalization [48]. Alternative structures of the minimal-PBPK models were assessed such as numbers of tissue compartments, the same or different K_p values, and the same or different f_{di} values for multiple tissue spaces.

Moxifloxacin PK after intravenous dosing in five species was simultaneously described by integrating allometric scaling principles into the minimal-PBPK model with one tissue compartment. The integrated model was described by:

$$Q_{CO}=0.275\cdot BW^{0.75} \quad (11)$$

$$CL=a\cdot BW^{b} \quad (12)$$

All species were assumed to have the same fitted f_d and K_p value, while Q_{CO} and CL were allometrically scaled across species [49, 50] with two estimated parameters for CL (a and b)

Human PK profiles for 6 mAb after intravenous dosing were fitted and compared between minimal-PBPK models with CL from either tissue or plasma compartments (Fig. 4).

Fittings utilized the maximum likelihood method in ADAPT 5 [51]. The variance model was defined as:

$$V_i=(\sigma_1+\sigma_2 Y(t_i))^2 \quad (13)$$

where V_i is the variance of the response at the ith time point, t_i is the actual time at the ith time point, and $Y(t_i)$ represents the predicted response at time t_i from the model. Variance parameters σ_1 and σ_2 were estimated together with system parameters during fittings. The goodness-of-fit criteria included visual inspection of the fitted curves, sum of squared residuals, Akaike Information Criterion (*AIC*), Schwarz Criterion (*SC*), and Coefficient of Variation (*CV*) of the estimated parameters.

Results

General evaluation

The first physiological feature of the minimal-PBPK model is the assignment of blood (or plasma) volume as the initial distribution space as is done in full PBPK models. This has worked well in numerous instances and obviates a major problem in mammillary models where early time extrapolations are dependent on the timing and frequency of blood sampling [2, 3]. The assigned blood (or plasma) volume can be more specific with considerations of species, sex, and age differences [52]. The assumed blood volume for man was 5.2 L/70 kg [49].

The second feature is the employment of Fick's Law of Perfusion for tissue distribution with the capability of tissue drug uptake and release to be either flow- or permeability-limited and limited to passive mechanisms. The $f_{di}\cdot Q_{CO}$ parameter, equivalent to distribution clearance, uses an assumed Q_{CO} (for man, 5.6 L/min) as do PBPK models. The fraction f_{di} allows for either multiple tissues and/or limitations in either capillary or cellular permeability. The structural or boundary limitation of $f_{d1} + f_{d2} \leq 1$ is needed.

A key aspect of PBPK models is assessment of tissue/plasma partition coefficients by direct measurements. Mammillary models yield a tissue-average K_p value from V_{ss}/BW [53]. The minimal-PBPK models incorporate one or more K_p values as fitted parameters.

Full PBPK models use actual organ and tissue weights in assessing overall distribution of drug, often requiring a carcass or 'residual' weight to account for unsampled sites. The minimal-PBPK models set BW or $ECF = V_1 + V_2 + V_p$. Here, the values of these parameters are assigned as physical volumes (or masses) of tissues (for man, BW = 70 kg). In certain cases, V_1 (or V_2) can be designated as a specific tissue. For instance, muscle accounts for 40–45 % of total body mass [49]; designating muscle as V_1 (or V_2) along with $f_d\cdot Q_{CO}$ for its blood flow is feasible. In some situations (beta-lactams), the total distribution space is known to be ECF [54]. Of course, more specific values of all physiological parameters can be matched to actual subject characteristics.

The extended model with hepatic compartment allows separate estimates of CL_{intu} and $CL_{non\text{-}hep}$. In certain cases, one clearance can be neglected if the other dominates. If the liver only slightly contributes to overall clearance, then including the hepatic compartment becomes futile and the extended model reduces to the basic model (Fig. 2).

It is feasible to incorporate hepatic intrinsic clearance and renal clearance as in full PBPK models. Tissue intrinsic clearances are easier to match to in vitro observations and have higher scaling potential to other species than systemic clearance [55]. A basic model

assigning CL to the tissue compartment may reflect underlying mechanisms of drug elimination and permit estimates of an average tissue 'intrinsic' clearance.

Beta-lactam antibiotics

The PK of 22 beta-lactam antibiotics were found in the literature and their profiles were analyzed based on the proposed minimal-PBPK models. The final structural model was defined with the same K_p for two tissue compartments for 12 beta-lactam antibiotics. The remaining 10 drugs were described by a model with one tissue compartment. Total volume $V_p + V_1 + V_2$ was assumed to be ECF in this analysis (volume = 18.2 L) because beta-lactam antibiotics distribute mainly within extracellular fluid [54]. The fitted profiles are shown in Fig. 5 and the parameters are summarized in Table 1. All models captured the observed PK profiles quite well with reasonable CV % for the estimated parameters.

For most beta-lactam antibiotics, tissue distribution rates were much lower than cardiac output ($f_{d1} + f_{d2} < 1$); indicating permeability-limited uptake.

The K_p values were also calculated separately according to $K_p = f_{up}/f_{ue}$ using the relationship for fraction unbound in interstitial fluid (ISF):

$$f_{ue} = 1/(1 + E/P \cdot (1 - f_{up})/f_{up}) \quad (14)$$

where E/P is the ratio of protein concentrations for ISF: plasma and f_{ue} was approximated assuming albumin concentration in ISF being half that present in plasma [56]. The estimated K_p obtained by minimal-PBPK modeling correlated roughly ($r^2 = 0.319$) with the calculated K_p (Fig. 6). This suggests that the unbound fraction only partly influences the degree to which beta-lactam antibiotics penetrate into interstitial fluids [57]. Other factors may also contribute such as ionization [58], transporters [59], or binding to other macromolecules such as penicillin-binding proteins [60]. Table 1 lists V_{ss} values calculated by $V_{ss} = V_p + \Sigma K_{pi} \cdot V_{ti}$.

Hepatic elimination drugs

Four drugs with hepatic first-pass effects and incomplete apparent bioavailability (Bio) were selected for this analysis: dihydrocodeine [37], verapamil [38], repaglinide [39], and midazolam [40]. The data in the literature included both IV and oral administration. The extended model with the hepatic compartment and with typical Q_{hep} and V_{hep} values [49] was used to analyze these data. The assumed Q_{hep} was 1.45 L/min in man and 9.8 mL/min in rat [49]. As shown in Fig. 7, there is good agreement between the observed data and model-predicted profiles. The estimated parameters are listed in Table 2.

Dihydrocodeine—The PK studies of dihydrocodeine were conducted in healthy subjects by Rowell et al. [37]. The extended model simultaneously captured the PK profiles following oral and IV dosing (Fig. 7). The finding that $f_{d1} + f_{d2} = 1$ indicates that dihydrocodeine rapidly diffuses into tissues with uptake restricted by blood flow. Hepatic intrinsic clearance is 0.424 L/min and $CL_{hep} = 0.328$ L/min. The hepatic extraction ratio (ER) was calculated according to Eq. 8 as 0.245 and F_G was estimated as 0.409. Thus, overall bio-availability would be about 0.309 based upon $F_G \cdot (1\text{-}ER)$, near to the NCA Bio value of 0.266. Dihydrocodeine is known to be extensively metabolized in the liver and the modeling results support this with a negligible estimate of $CL_{non\text{-}hep}$. The separate estimates of different clearances allow quantitative assessment of their relative contributions to drug elimination and also support an identifiable F_G.

Verapamil—Hepatic metabolism is the predominant route of elimination for verapamil and almost no intact drug is excreted according to previous studies [61]. The model supported this with a small estimate of $CL_{non\text{-}hep}$ as 0.214 L/min. Figure 7 shows the fitted results. CL_{intu} is 1.34 L/min, CL_{hep} = 0.696 L/min, and ER was 0.520. High hepatic extraction resulted in low systemic bioavailability (26.6 %), in line with a previous study and the NCA Bio of 0.217 [62]. The high estimate of $f_{d1} + f_{d2}$ indicates that the permeability of verapamil across capillary and cellular membranes was very high and distribution rate is primarily controlled by blood flow.

Repaglinide—This PK study of repaglinide was conducted in rats. Figure 7 shows the fitted results. A previous study indicated that repaglinide is mainly excreted via bile into feces and hepatic clearance dominates the overall elimination [63]. Our analysis confirmed this. The F_G was 0.5, multiplying 1-ER (0.148), gives an overall bioavailability of 0.426. The high estimate of $f_{d1} + f_{d2}$ suggested that distribution rate is mainly controlled by blood flow.

Midazolam—As a probe of CYP450 3A4/5, midazolam is subject to extensive first-pass metabolism in both intestine and liver [64]. Several approaches have evaluated the relative contributions of intestinal and hepatic metabolism to the overall first-pass effect [65, 66]. The fitted profiles are shown in Fig. 7. Our modeling gave estimates of their contributions. The F_G was 0.742 and liver ER is 0.329, indicating comparable first-pass effects from intestine and liver. Such first-pass effect was also observed in previous studies [65, 66]. The K_p was about 0.655, consistent with an average PBPK literature value [67]. Hepatic and intestinal clearance accounts for most drug elimination as no other clearance was detected in our analysis.

Inter-species PK of moxifloxacin

As shown in Fig. 8, the PK of moxifloxacin in five species was assessed simultaneously by the integrated minimal-PBPK model. The estimated parameters are listed in Table 3. The low CV % values for the parameter estimates indicate good model performance although fittings for some of the digitized data are only approximate. Moxifloxacin appears to efficiently penetrate into tissues with blood flow as the rate-limiting step in the distribution process for the five species as shown by the high f_d value of 1.0. The exponent (b) of the allometric equation for CL was 0.591, close to a reported value [68]. The K_p was 2.70, indicating moderate tissue partitioning and consistent with average tissue concentration in rats [69]. The initial misfit of the last several points for man observed in Fig. 8 may indicate that of CL does not precisely follow a conventional allometric relationship (Eq. 12). The fitting of human data was improved when b was increased. It is well appreciated that CL in man sometimes needs modifications from expectations of preclinical data. The main point of this case was to show a global mPBPK approach to assess f_d and K_p, as well as scale CL across species.

Monoclonal antibodies

The clinical PK studies of six mAb were selected for this analysis: Hu12F6mu [42], lexatumumab [43], MEDI-528 [44], MEDI-563 [45], CR002 [46] and pateclizumab [47]. All mAb selected in this analysis showed linear PK that is usually analyzed with a 2CM mammillary model. The fitted profiles and simulated tissue concentrations are shown in Fig. 9 and the parameters are listed in Table 4 for models with tissue (Model A) versus plasma clearance (Model B). The models captured the observed PK profiles quite well with precise estimates of parameters. The tissue: plasma exposure ratios (AUC ratios) are reflected by the K_p values, which ranged 0.0475–0.0664 with Model A, and ranged 0.0330–0.0429 with Model B. Studies in mice have shown the muscle: serum AUC ratio of an antiplatelet

antibody 7E3 to be 0.038, while other tissues had AUC ratios of 0.125 ± 0.036 [70]. Since muscle is about 60 % of BW, the mass-average AUC ratio should be about 0.07. A study in patients observed similar tissue: plasma AUC ratios of ^{111}In-labeled ZCEO25 IgG [71]. Thus, Model A appears somewhat superior to Model B. Both models yielded low estimates of f_d, and Model A yielded f_d in the range of 1.1–11.1 × 10^{-4}. This gives a vascular permeability (f_d·Q_{CO}) in the range of 0.017–0.17, close to a permeability value of 0.00567 L/h/70 kg (PS_L + PS_S) employed in a PBPK model by Baxter et al. [71]. mAbs are subject to extremely low capillary permeability [72] and net tissue uptake is further diminished by FcRn recycling [73]. Predictions of functional tissue concentrations of mAb should preferably employ interstitial fluid volume for V_t rather than $BW - V_p$ owing to their limited cellular uptake except when a cellular target or receptor exists [71]. These models could be readily adapted to handle target-mediated disposition in plasma [74] or in tissue [75].

Discussion

Full PBPK models use the modeling paradigm depicted in Fig. 1 melding all known body and drug properties to either simulate expected concentration–time profiles or perform fittings of available data. Blood flows and organ/tissue weights are largely taken from literature sources [49]. The PBPK models thus either confirm basic expectations about drug disposition or reveal further complexities where investigators add new model features based on experimental data and/or reasonable assumptions.

Minimal PBPK models offer similar possibilities with the constraints of only assessing blood or plasma concentration versus time data and yielding tissue-average drug concentrations. Our case studies with an array of drugs and disposition profiles allowed for reasonable fittings of data with model features predicated on the physicochemical and metabolic properties of a variety of drugs but providing outcomes with low dimensionality and ease of interpretation. As with full PBPK models, there is flexibility in adjusting major model components to accommodate specific drugs and conditions. The parameter estimates can be interpreted with more realism than compartmental models.

The purpose of this report is to demonstrate how minimal PBPK models can be envisioned and applied. The data were all digitized and thus analysis results will be imperfect. Owing to differences in assumptions, the fittings and parameters may differ somewhat from use of compartment models.

As with full PBPK models, blood or plasma volume, cardiac output, and total body space (BW or ECF) are assumed physiological components. For more extensive data sets, these parameters could be specified for subjects of varying ages, sexes, and body weights [76]. This provides freedom to allow the data to reveal f_d, K_p, and CL values, parameters of special interest in PK. Most PK profiles are intrinsically bi- or tri-exponential allowing fitting of 4 or 6 parameters, both for compartmental models [2] as well as with minimal-PBPK models. Both approaches involve ‘lumping’ perspectives. When these models do not function well, there are likely added complexities which are not encompassed within the basic model structures and which need exploration.

Full PBPK, minimal-PBPK, and compartmental models have the expectation that $CL = Dose_{IV}/AUC$ when elimination occurs from blood or plasma. Compartmental models have the weakness that limited early blood sampling can miss high initial drug concentrations [77] and lead to deviations in estimates of the central compartment volume and cause bias of AUC prediction. For other clearance mechanisms, the minimal-PBPK models can easily

include the liver for assessment of first-pass effects when jointly fitting oral and IV data (Fig. 3) or tissue clearance can be implemented (Fig. 4).

Compartmental models (with plasma CL) yield a whole-body distribution coefficient, $K_p = V_{ss}/BW$ [53]. The same parameter can be generated from both full and minimal PBPK models from $V_{ss} = V_p + \Sigma K_{pi} \cdot V_{ti}$. The minimal-PBPK models provide one or two K_p values depending on the number of exponential phases in the data. This number and value(s) are determined in a trial-and-error fitting approach. Of advantage for interpretation, this parameter is directly revealed as one of the primary 'independent' variables for each drug. These K_p values reflect either fractional tissue spaces [78] and/or plasma and tissue binding and can be compared among congeneric drugs (beta-lactams, Table 1) or among species (moxifloxacin, Table 3). Scaling of animal data to man is readily feasible with minimal-PBPK models using aspects of allometry for select model components as was done for moxifloxacin.

The minimal-PBPK models are attractive in utilizing the well-known Fick's Law of Perfusion. The employment of the fractional distribution (f_d) parameter not only accounts for organ/tissue 'lumping', but allows for inaccuracies or variability in Q_{CO} as well as flexibility for distribution to be controlled by permeability as revealed by small values of f_d. The value of $f_d Q_{CO}$ is equivalent to distribution clearance (CL_D) as proposed by Stec and Atkinson [79] who adapted earlier concepts from the Kety–Renkin–Crone equation [80–83]:

$$CL_D = Q \cdot (1 - e^{-PS/Q}) \quad (15)$$

where Q is blood flow and PS is a permeability/surface area coefficient. The function allows the value of $CL_D \rightarrow Q$ when $PS \gg Q$ and $CL_D \rightarrow PS$ when $PS \gg Q$. Thus small values of f_d depict permeability-limited tissue access and reflect operation of Fick's Law of Diffusion. However, within the context of the minimal-PBPK paradigm, the f_d values may represent either differing blood distribution to tissues/organs and/or flow/permeability. Of course, the presence of transporters will complicate such assessment [84].

It has been somewhat surprising that full PBPK models commonly work well with use of blood flow to various organs and tissues with occasional introduction of PS values for interstitial-cell water distribution [85]. It has been long appreciated that capillary permeability varies with molecular size producing very slow tissue access for large molecules such as plasma proteins [86, 87]. More frequent model assessment should be done based on permeability-limited access for various molecules. The minimal-PBPK models provide f_d values allowing for a full range of PS and Q values to be operative for tissue distribution.

The parameters of minimal-PBPK models have a simple and logical basis allowing ease of fitting and interpretation. Preliminary NCA analysis can provide estimates of CL from $Dose/AUC$ and K_p from $V_{ss}/BW = MRT \cdot CL/BW$ where MRT is Mean Residence Time. Values of f_d must fall between 0 and 1 and both f_d and K_p are dimensionless. The value of V_1 must fall with $BW - V_p \geq V_1$. Thus, most model parameters have natural physiological limits with restricted parameter spaces allowing for robust parameter estimates. The opposite extreme exists with finding rate constants in compartmental models which are non-intuitive and range widely.

The minimal-PBPK models are highly flexible allowing for most of the modeling adjustments found in applying full-PBPK models. An infusion rate constant or Bischoff $g(t)$ input function [88] may be needed to mimic very early circulatory kinetics [6] rather than assuming Initial Conditions of $Dose/V_p$. The preferred organ perfusion medium is arterial

rather than venous blood [1–3], although this is seldom feasible in human studies. Our modeling employed venous drug concentrations which is also not uncommon in enacting full PBPK models.

The model with hepatic clearance involved use of the well-stirred model and assumptions that the K_p value of liver was the same as other tissues and intrinsic clearance acts on unbound drug in liver. Thus the calculated parameters would differ if another hepatic model was applied (e.g. parallel-tube), if differential tissue binding occurs, and if facilitated uptake or nonrestrictive metabolism was present [89, 90]. Most of our conditions are commonly applied in full PBPK models.

The site of drug administration (IV, IM, SC, oral) can be more relevant than in compartmental models as shown with the extended model (Fig. 3). Nonlinearity in CL or K_p can be added when the range of doses, drug properties, and data profiles allow. As demonstrated with our cases, greater modeling flexibility is gained when studies include diverse dosing (Fig. 7), species (Fig. 8), or experimental conditions (Figs. 5, 9).

The present demonstration of various applications of minimal PBPK modeling utilized digitized data from various literature sources. Thus the parameter estimates are approximate but clearly reflect the feasibility of this modeling approach. However, as a fifth example of minimal-PBPK modeling with more comprehensive metrics, Grimsrud et al. [91] successfully applied a model similar to that in Fig. 2 to assess detomidine PK after IV and IM doses in horses using a population approach with specific physiological parameters for each horse. A physiologic muscle compartment was employed for V_2 as the site of IM drug administration.

Application of full PBPK models remains the gold standard in PK, but requires physicochemical, physiologic, animal tissue, and in vitro metabolic measurements along with appreciable modeling efforts. Minimal-PBPK models offer a sensible compromise when only blood or plasma data are available. They allow the insightful pharmacokineticist great liberties in evaluating data and providing parameters of practical value.

Acknowledgments

This research was supported by the National Institutes of Health Grant GM57980, the University at Buffalo—Pfizer Strategic Alliance, and the UB Center for Protein Therapeutics. Review of this manuscript by Drs. Sihem Ait-Oudhia, Peter Bonate, Wilhelm Huisinga, Wojciech Krzyzanski, Donald E. Mager, and Marilyn E. Morris is appreciated.

References

1. Rowland M, Peck C, Tucker G. Physiologically-based pharmacokinetics in drug development and regulatory science. Annu Rev Pharmacol Toxicol. 2011; 51:45–73. [PubMed: 20854171]
2. Jusko, WJ. Guidelines for collection and pharmacokinetic analysis of drug disposition data. In: Evans, WE.; Schentag, JJ.; Jusko, WJ., editors. Applied pharmacokinetics: principles of therapeutic drug monitoring. 1. Applied Therapeutics Inc; Vancouver, WA: 1980. p. 639-680.
3. Chiou WL. Potential pitfalls in the conventional pharmacokinetic studies: effects of the initial mixing of drug in blood and the pulmonary first-pass elimination. J Pharmacokinet Biopharm. 1979; 7:527–536. [PubMed: 529021]
4. Riegelman S, Loo JC, Rowland M. Shortcomings in pharmacokinetic analysis by conceiving the body to exhibit properties of a single compartment. J Pharm Sci. 1968; 57:117–123. [PubMed: 5652110]
5. Vaughan DP, Hope I. Applications of a recirculatory stochastic pharmacokinetic model: limitations of compartmental models. J Pharmacokinet Biopharm. 1979; 7:207–225. [PubMed: 20218015]

6. Krejcie TC, Henthorn TK, Shanks CA, Avram MJ. A recirculatory pharmacokinetic model describing the circulatory mixing, tissue distribution and elimination of antipyrine in dogs. J Pharmacol Exp Ther. 1994; 269:609–616. [PubMed: 8182527]
7. Veng-Pedersen P, Freise KJ, Schmidt RL, Widness JA. Pharmacokinetic differentiation of drug candidates using system analysis and physiological-based modelling. Comparison of C.E.R.A. and erythropoietin. J Pharm Pharmacol. 2008; 60:1321–1334. [PubMed: 18812025]
8. Nestorov IA, Aarons LJ, Arundel PA, Rowland M. Lumping of whole-body physiologically based pharmacokinetic models. J Pharmacokinet Biopharm. 1998; 26:21–46. [PubMed: 9773391]
9. Pilari S, Huisinga W. Lumping of physiologically-based pharmacokinetic models and a mechanistic derivation of classical compartmental models. J Pharmacokinet Pharmacodyn. 2010; 37:365–405. [PubMed: 20661651]
10. Levy G, Mager DE, Cheung WK, Jusko WJ. Comparative pharmacokinetics of coumarin anticoagulants L: physiologic modeling of S-warfarin in rats and pharmacologic target-mediated warfarin disposition in man. J Pharm Sci. 2003; 92:985–994. [PubMed: 12712418]
11. Kawahara M, Sakata A, Miyashita T, Tamai I, Tsuji A. Physiologically based pharmacokinetics of digoxin in mdr1a knockout mice. J Pharm Sci. 1999; 88:1281–1287. [PubMed: 10585223]
12. Rocci ML Jr, Szefler SJ, Acara M, Jusko WJ. Prednisolone metabolism and excretion in the isolated perfused rat kidney. Drug Metab Dispos. 1981; 9:177–182. [PubMed: 6113924]
13. Gallo JM, Vicini P, Orlansky A, Li S, Zhou F, Ma J, Pulfer S, Bookman MA, Guo P. Pharmacokinetic model-predicted anticancer drug concentrations in human tumors. Clin Cancer Res. 2004; 10:8048–8058. [PubMed: 15585640]
14. Henthorn TK, Avram MJ, Krejcie TC, Shanks CA, Asada A, Kaczynski DA. Minimal compartmental model of circulatory mixing of indocyanine green. Am J Physiol. 1992; 262:H903–H910. [PubMed: 1558199]
15. Rowland M, Benet LZ, Graham GG. Clearance concepts in pharmacokinetics. J Pharmacokinet Biopharm. 1973; 1:123–136. [PubMed: 4764426]
16. Lobo ED, Hansen RJ, Balthasar JP. Antibody pharmacokinetics and pharmacodynamics. J Pharm Sci. 2004; 93:2645–2668. [PubMed: 15389672]
17. Humbert G, Spyker DA, Fillastre JP, Leroy A. Pharmacokinetics of amoxicillin: dosage nomogram for patients with impaired renal function. Antimicrob Agents Chemother. 1979; 15:28–33. [PubMed: 426503]
18. Champoux N, Du Souich P, Ravaoarinoro M, Phaneuf D, Latour J, Cusson JR. Single-dose pharmacokinetics of ampicillin and tobramycin administered by hypodermoclysis in young and older healthy volunteers. Br J Clin Pharmacol. 1996; 42:325–331. [PubMed: 8877023]
19. Pfeffer M, Gaver RC, Ximenez J. Human intravenous pharmacokinetics and absolute oral bioavailability of cefatrizine. Antimicrob Agents Chemother. 1983; 24:915–920. [PubMed: 6660858]
20. Lee FH, Pfeffer M, Van Harken DR, Smyth RD, Hottendorf GH. Comparative pharmacokinetics of ceforanide (BL-S786R) and cefazolin in laboratory animals and humans. Antimicrob Agents Chemother. 1980; 17:188–192. [PubMed: 7387141]
21. Lofgren S, Bucht G, Hermansson B, Holm SE, Winblad B, Norrby SR. Single-dose pharmacokinetics of dicloxacillin in healthy subjects of young and old age. Scand J Infect Dis. 1986; 18:365–369. [PubMed: 3764352]
22. Landersdorfer CB, Kirkpatrick CM, Kinzig-Schippers M, Bulitta JB, Holzgrabe U, Drusano GL, Sorgel F. Population pharmacokinetics at two dose levels and pharmacodynamic pro-filing of flucloxacillin. Antimicrob Agents Chemother. 2007; 51:3290–3297. [PubMed: 17576847]
23. Gambertoglio JG, Barriere SL, Lin ET, Conte JE Jr. Pharmacokinetics of mecillinam in health subjects. Antimicrob Agents Chemother. 1980; 18:952–956. [PubMed: 6263180]
24. Bulitta JB, Duffull SB, Kinzig-Schippers M, Holzgrabe U, Stephan U, Drusano GL, Sorgel F. Systematic comparison of the population pharmacokinetics and pharmacodynamics of piperacillin in cystic fibrosis patients and healthy volunteers. Antimicrob Agents Chemother. 2007; 51:2497–2507. [PubMed: 17485505]
25. Hampel B, Feike M, Koeppe P, Lode H. Pharmacokinetics of temocillin in volunteers. Drugs. 1985; 29(Suppl 5):99–102. [PubMed: 4029032]

26. Frimodt-Moller N, Maigaard S, Toothaker RD, Bundtzen RW, Brodey MV, Craig WA, Welling PG, Madsen PO. Mezlocillin pharmacokinetics after single intravenous doses to patients with varying degrees of renal function. Antimicrob Agents Chemother. 1980; 17:599–607. [PubMed: 6446877]
27. Vinge E, Nergelius G, Nilsson LG, Lidgren L. Pharmacokinetics of cloxacillin in patients undergoing hip or knee replacement. Eur J Clin Pharmacol. 1997; 52:407–411. [PubMed: 9272413]
28. Yaffe SJ, Gerbracht LM, Mosovich LL, Mattar ME, Danish M, Jusko WJ. Pharmacokinetics of methicillin in patients with cystic fibrosis. J Infect Dis. 1977; 135:828–831. [PubMed: 404369]
29. Rumble RH, Roberts MS, Scott AR. The effect of posture on the pharmacokinetics of intravenous benzylpenicillin. Eur J Clin Pharmacol. 1986; 30:731–734. [PubMed: 3770066]
30. Meyers BR, Hirschman SZ, Strougo L, Srulevitch E. Comparative study of piperacillin, ticarcillin, and carbenicillin pharmacokinetics. Antimicrob Agents Chemother. 1980; 17:608–611. [PubMed: 6446878]
31. Kikuchi E, Kikuchi J, Nasuhara Y, Oizumi S, Ishizaka A, Nishimura M. Comparison of the pharmacodynamics of biapenem in bronchial epithelial lining fluid in healthy volunteers given half-hour and three-hour intravenous infusions. Antimicrob Agents Chemother. 2009; 53:2799–2803. [PubMed: 19380601]
32. Colaizzi PA, Polk RE, Poynor WJ, Raffalovich AC, Cefali EA, Beightol LA. Comparative pharmacokinetics of azlocillin and piperacillin in normal adults. Antimicrob Agents Chemother. 1986; 29:938–940. [PubMed: 3729353]
33. Barza M, Melethil S, Berger S, Ernst EC. Comparative pharmacokinetics of cefamandole, cephapirin, and cephalothin in healthy subjects and effect of repeated dosing. Antimicrob Agents Chemother. 1976; 10:421–425. [PubMed: 984783]
34. Kampf D, Schurig R, Korsukewitz I, Bruckner O. Cefoxitin pharmacokinetics: relation to three different renal clearance studies in patients with various degrees of renal insufficiency. Antimicrob Agents Chemother. 1981; 20:741–746. [PubMed: 7325641]
35. Waller ES, Sharanevych MA, Yakatan GJ. The effect of probenecid on nafcillin disposition. J Clin Pharmacol. 1982; 22:482–489. [PubMed: 7174857]
36. Dudley MN, Shyu WC, Nightingale CH, Quintiliani R. Effect of saturable serum protein binding on the pharmacokinetics of unbound cefonicid in humans. Antimicrob Agents Chemother. 1986; 30:565–569. [PubMed: 3789691]
37. Rowell FJ, Seymour RA, Rawlins MD. Pharmacokinetics of intravenous and oral dihydrocodeine and its acid metabolites. Eur J Clin Pharmacol. 1983; 25(3):419–424. [PubMed: 6628531]
38. Krecic-Shepard ME, Barnas CR, Slimko J, Jones MP, Schwartz JB. Gender-specific effects on verapamil pharmacokinetics and pharmacodynamics in humans. J Clin Pharmacol. 2000; 40:219–230. [PubMed: 10709150]
39. Li C, Choi DH, Choi JS. Effects of efonidipine on the pharmacokinetics and pharmacodynamics of repaglinide: possible role of CYP3A4 and P-glycoprotein inhibition by efonidipine. J Pharmacokinet Pharmacodyn. 2012; 39:99–108. [PubMed: 22210483]
40. Heizmann P, Eckert M, Ziegler WH. Pharmacokinetics and bioavailability of midazolam in man. Br J Clin Pharmacol. 1983; 16(Suppl 1):43S–49S. [PubMed: 6138080]
41. Siefert HM, Domdey-Bette A, Henninger K, Hucke F, Kohls-dorfer C, Stass HH. Pharmacokinetics of the 8-meth-oxyquinolone, moxifloxacin: a comparison in humans and other mammalian species. J Antimicrob Chemother. 1999; 43(Suppl B):69–76. [PubMed: 10382878]
42. Li J, Zhou B, Shentu J, Du L, Tan M, Hou S, Qian W, Li B, Zhang D, Dai J, Wang H, Zhang X, Chen J, Guo Y. Phase I trial of a humanized, Fc receptor nonbinding anti-CD3 antibody, hu12F6mu in patients receiving renal allografts. MAbs. 2010; 2:449–456.
43. Wakelee HA, Patnaik A, Sikic BI, Mita M, Fox NL, Miceli R, Ullrich SJ, Fisher GA, Tolcher AW. Phase I and pharmacokinetic study of lexatumumab (HGS-ETR2) given every 2 weeks in patients with advanced solid tumors. Ann Oncol. 2010; 21:376–381. [PubMed: 19633048]
44. White B, Leon F, White W, Robbie G. Two first-in-human, open-label, phase I dose-escalation safety trials of MEDI-528, a monoclonal antibody against interleukin-9, in healthy adult volunteers. Clin Ther. 2009; 31:728–740. [PubMed: 19446146]

45. Busse WW, Katial R, Gossage D, Sari S, Wang B, Kolbeck R, Coyle AJ, Koike M, Spitalny GL, Kiener PA, Geba GP, Molfino NA. Safety profile, pharmacokinetics, and biologic activity of MEDI-563, an anti-IL-5 receptor alpha antibody, in a phase I study of subjects with mild asthma. J Allergy Clin Immunol. 2010; 125(1237–1244):e1232.
46. Hawthorne T, Giot L, Blake L, Kuang B, Gerwien R, Smithson G, Hahne W, Mansfield T, Starling GC, Pochart P, Hoelscher D, Halvorsen YD. A phase I study of CR002, a fully-human monoclonal antibody against platelet-derived growth factor-D. Int J Clin Pharmacol Ther. 2008; 46:236–244. [PubMed: 18538109]
47. Emu B, Luca D, Offutt C, Grogan JL, Rojkovich B, Williams MB, Tang MT, Xiao J, Lee JH, Davis JC. Safety, pharmacokinetics, and biologic activity of pateclizumab, a novel monoclonal antibody targeting lymphotoxin alpha: results of a phase I randomized, placebo-controlled trial. Arthritis Res Ther. 2012; 14:R6. [PubMed: 22225620]
48. Rodionov, N. Graph digitizer version 1.9. 2000. http://www.geocities.com/graphdigitizer
49. Brown RP, Delp MD, Lindstedt SL, Rhomberg LR, Beliles RP. Physiological parameter values for physiologically based pharmacokinetic models. Toxicol Ind Health. 1997; 13:407–484. [PubMed: 9249929]
50. Boxenbaum H. Interspecies scaling, allometry, physiological time, and the ground plan of pharmacokinetics. J Pharmacokinet Biopharm. 1982; 10:201–227. [PubMed: 7120049]
51. D'Argenio, DZ.; Schumitzky, A.; Wang, XN. ADAPT V user's guide: pharmacokinetic/pharmacodynamic system analysis software, biomedical simulations resource. Los Angeles: 2009.
52. ICRP Publication 89. Basic anatomical and physiological data for use in radiological protection: reference values. A report of age- and gender-related differences in the anatomical and physiological characteristics of reference individuals. Ann ICRP. 2002; 32(3–4):5–265. [PubMed: 14506981]
53. Jusko WJ, Chiang ST. Distribution volume related to body weight and protein binding. J Pharm Sci. 1982; 71:469–470. [PubMed: 7086663]
54. Cars O. Pharmacokinetics of antibiotics in tissues and tissue fluids: a review. Scand J Infect Dis Suppl. 1990; 74:23–33. [PubMed: 2097711]
55. Shiran MR, Proctor NJ, Howgate EM, Rowland-Yeo K, Tucker GT, Rostami-Hodjegan A. Prediction of metabolic drug clearance in humans: in vitro-in vivo extrapolation vs allometric scaling. Xenobiotica. 2006; 36:567–580. [PubMed: 16864504]
56. McNamara PJ, Gibaldi M, Stoeckel K. Fraction unbound in interstitial fluid. J Pharm Sci. 1983; 72:834–836. [PubMed: 6886999]
57. Wise R, Gillett AP, Cadge B, Durham SR, Baker S. The influence of protein binding upon tissue fluid levels of six beta-lactam antibiotics. J Infect Dis. 1980; 142:77–82. [PubMed: 7400630]
58. Barza M, Weinstein L. Some determinants of the distribution of penicillins and cephalosporins in the body. Practical and theoretical considerations. Ann N Y Acad Sci. 1974; 235:613–620. [PubMed: 4527978]
59. Fujiwara K, Shin M. Immunocytochemistry for amoxicillin and its use for studying uptake of the drug in the intestine, liver, and kidney of rats. Antimicrob Agents Chemother. 2011; 55(1):62–71. [PubMed: 20974868]
60. Griaznova NS, Subbotina NA. Penicillin-binding proteins. Their enzymatic activity and properties. Antibiot Med Biotekhnol. 1986; 31(7):487–498. [PubMed: 3532933]
61. Hamann SR, Blouin RA, McAllister RG Jr. Clinical pharmacokinetics of verapamil. Clin Pharmacokinet. 1984; 9:26–41. [PubMed: 6362951]
62. Eichelbaum M, Mikus G, Vogelgesang B. Pharmacokinetics of (+)-, (−)- and (±)-verapamil after intravenous administration. Br J Clin Pharmacol. 1984; 17:453–458. [PubMed: 6721991]
63. Sjogren E, Bredberg U, Lennernas H. The pharmacokinetics and hepatic disposition of repaglinide in pigs: mechanistic modeling of metabolism and transport. Mol Pharm. 2012; 9:823–841. [PubMed: 22352317]
64. Lin YS, Dowling AL, Quigley SD, Farin FM, Zhang J, Lamba J, Schuetz EG, Thummel KE. Co-regulation of CYP3A4 and CYP3A5 and contribution to hepatic and intestinal midazolam metabolism. Mol Pharmacol. 2002; 62:162–172. [PubMed: 12065767]

65. Tsunoda SM, Velez RL, von Moltke LL, Greenblatt DJ. Differentiation of intestinal and hepatic cytochrome P450 3A activity with use of midazolam as an in vivo probe: effect of ketoconazole. Clin Pharmacol Ther. 1999; 66:461–471. [PubMed: 10579473]

66. Thummel KE, O'Shea D, Paine MF, Shen DD, Kunze KL, Perkins JD, Wilkinson GR. Oral first-pass elimination of midazolam involves both gastrointestinal and hepatic CYP3A-mediated metabolism. Clin Pharmacol Ther. 1996; 59:491–502. [PubMed: 8646820]

67. Bjorkman S, Wada DR, Berling BM, Benoni G. Prediction of the disposition of midazolam in surgical patients by a physiologically based pharmacokinetic model. J Pharm Sci. 2001; 90:1226–1241. [PubMed: 11745776]

68. Cox SK. Allometric scaling of marbofloxacin, moxifloxacin, danofloxacin and difloxacin pharmacokinetics: a retrospective analysis. J Vet Pharmacol Ther. 2007; 30:381–386. [PubMed: 17803728]

69. Beckmann J, Kees F, Schaumburger J, Kalteis T, Lehn N, Grifka J, Lerch K. Tissue concentrations of vancomycin and moxifloxacin in periprosthetic infection in rats. Acta Orthop. 2007; 78:766–773. [PubMed: 18236182]

70. Garg A, Balthasar JP. Physiologically-based pharmacokinetic (PBPK) model to predict IgG tissue kinetics in wild-type and FcRn-knockout mice. J Pharmacokinet Pharmacodyn. 2007; 34:687–709. [PubMed: 17636457]

71. Baxter LT, Zhu H, Mackensen DG, Butler WF, Jain RK. Biodistribution of monoclonal antibodies: scale-up from mouse to human using a physiologically based pharmacokinetic model. Cancer Res. 1995; 55:4611–4622. [PubMed: 7553638]

72. Rippe B, Haraldsson B. Transport of macromolecules across microvascular walls: the two-pore theory. Physiol Rev. 1994; 74:163–219. [PubMed: 8295933]

73. Junghans RP. Finally! The Brambell receptor (FcRB). Mediator of transmission of immunity and protection from catabolism for IgG. Immunol Res. 1997; 16:29–57. [PubMed: 9048207]

74. Hayashi N, Tsukamoto Y, Sallas WM, Lowe PJ. A mechanism-based binding model for the population pharmacokinetics and pharmacodynamics of omalizumab. Br J Clin Pharmacol. 2007; 63:548–561. [PubMed: 17096680]

75. Lammerts van Bueren JJ, Bleeker WK, Bogh HO, Houtkamp M, Schuurman J, van de Winkel JG, Parren PW. Effect of target dynamics on pharmacokinetics of a novel therapeutic antibody against the epidermal growth factor receptor: implications for the mechanisms of action. Cancer Res. 2006; 66:7630–7638. [PubMed: 16885363]

76. Huisinga W, Solms A, Fronton L, Pilari S. Modeling interindividual variability in physiologically based pharmacokinetics and its link to mechanistic covariate modeling. Pharmacometrics Syst Pharmacol. 2012; 1:e4.

77. Weiss M. Modelling of initial distribution of drugs following intravenous bolus injection. Eur J Clin Pharmacol. 1983; 24:121–126. [PubMed: 6832194]

78. Levitt DG. The pharmacokinetics of the interstitial space in humans. BMC Clin Pharmacol. 2003; 3:3–14. [PubMed: 12890292]

79. Stec GP, Atkinson AJ Jr. Analysis of the contributions of permeability and flow of intercompartmental clearance. J Pharmacokinet Biopharm. 1981; 9:167–180. [PubMed: 7277207]

80. Kety SS. The theory and applications of the exchange of inert gas at the lungs and tissues. Pharmacol Rev. 1951; 3:1–41. [PubMed: 14833874]

81. Renkin EM. Effects of blood flow on diffusion kinetics in isolated, perfused hindlegs of cats; a double circulation hypothesis. Am J Physiol. 1955; 183:125–136. [PubMed: 13268649]

82. Renkin EM. Transport of potassium-42 from blood to tissue in isolated mammalian skeletal muscles. Am J Physiol. 1959; 197:1205–1210. [PubMed: 14437359]

83. Crone C. The permeability of capillaries in various organs as determined by use of the 'Indicator diffusion' method. Acta Physiol Scand. 1963; 58:292–305. [PubMed: 14078649]

84. Watanabe T, Kusuhara H, Sugiyama Y. Application of physiologically based pharmacokinetic modeling and clearance concept to drugs showing transporter-mediated distribution and clearance in humans. J Pharmacokinet Pharmacodyn. 2010; 37:575–590. [PubMed: 21063755]

85. Thompson MD, Beard DA. Development of appropriate equations for physiologically based pharmacokinetic modeling of permeability-limited and flow-limited transport. J Pharmacokinet Pharmacodyn. 2011; 38:405–421. [PubMed: 21584718]

86. Goldstein, A.; Aronow, L.; Kalman, SM. Principles of drug action: the basis of pharmacology. Harper & Row; New York: 1974. p. 147

87. Renkin EM. Multiple pathways of capillary permeability. Circ Res. 1977; 41:735–743. [PubMed: 923024]

88. Bischoff KB, Dedrick RL, Zaharko DS, Longstreth JA. Methotrexate pharmacokinetics. J Pharm Sci. 1971; 60:1128–1133. [PubMed: 5127083]

89. Poulin P, Kenny JR, Hop CE, Haddad S. In vitro–in vivo extrapolation of clearance: modeling hepatic metabolic clearance of highly bound drugs and comparative assessment with existing calculation methods. J Pharm Sci. 2012; 101:838–851. [PubMed: 22009717]

90. Chiba M, Ishii Y, Sugiyama Y. Prediction of hepatic clearance in human from in vitro data for successful drug development. AAPS J. 2009; 11:262–276. [PubMed: 19408130]

91. Grimsrud, KN.; Ait-Oudhia, S.; Durbin-Johnson, BP.; Rocke, DM.; Mama, KR.; Rezende, ML.; Stanley, SD.; Jusko, WJ. Population pharmacokinetic and pharmacodynamic analysis comparing diverse effects of detomidine, medetomidine and dexmedetomidine in the horse; Presented at the Annual Symposium of the Veterinary Science Training Program; University of California, Davis. March 2012; 2012.

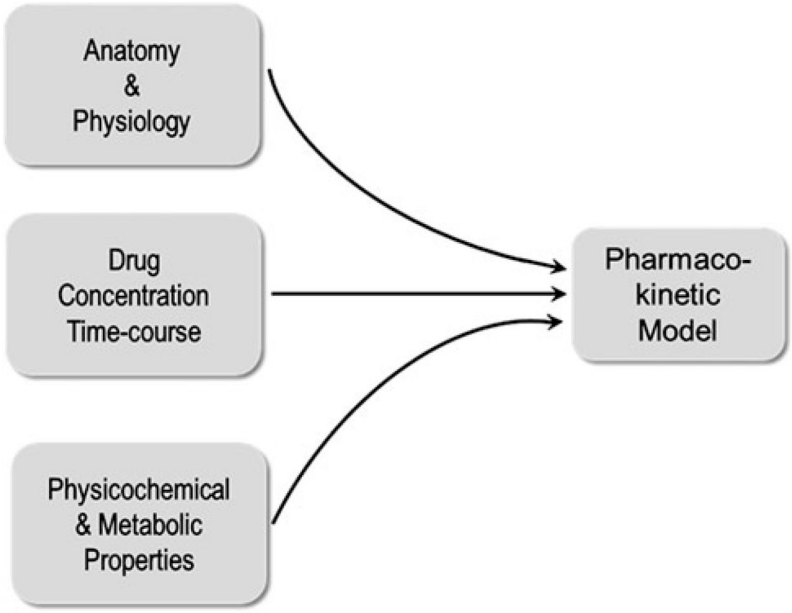

Fig. 1.
Paradigm for constructing PBPK models

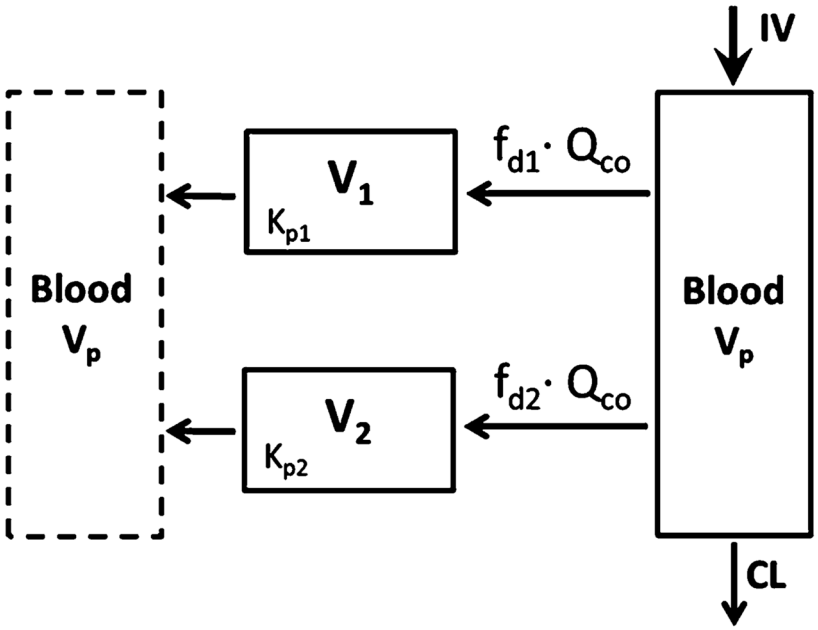

Fig. 2.
Minimal-PBPK model with two tissue compartments. Symbols and physiological restrictions are defined with Eqs. (1–3). The blood compartment in the *left box* mimics the venous blood as in full PBPK models, but is not utilized in the present model

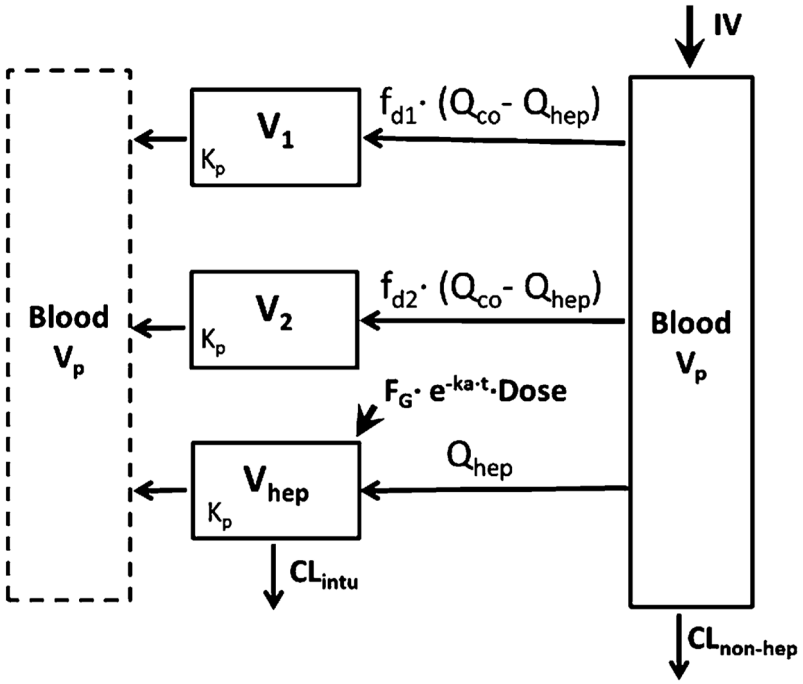

Fig. 3.
Minimal-PBPK model extended with the hepatic compartment. *Symbols* and physiological restrictions are defined in Table 2

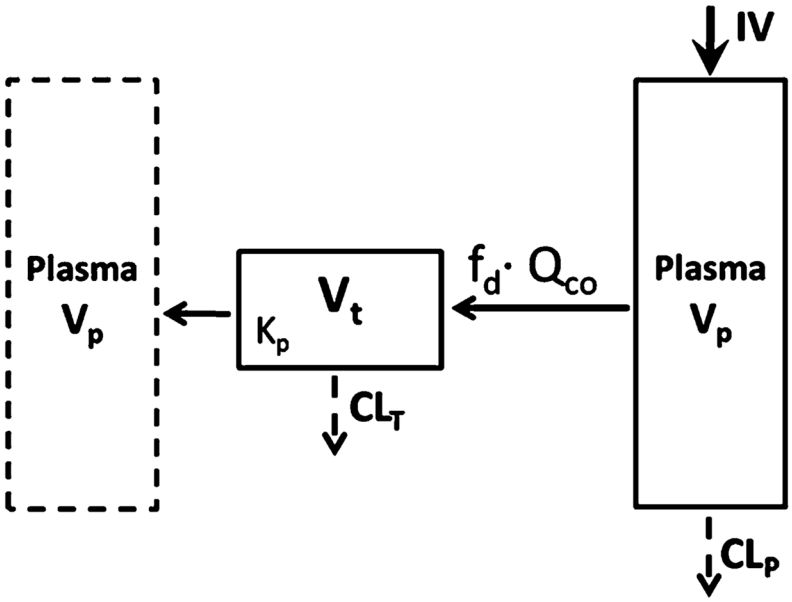

Fig. 4.
Basic minimal-PBPK model assigning *CL* either from tissue (Model A) or plasma compartments (Model B). *Symbols* and physiological restrictions are defined with Eqs. (9) and (10)

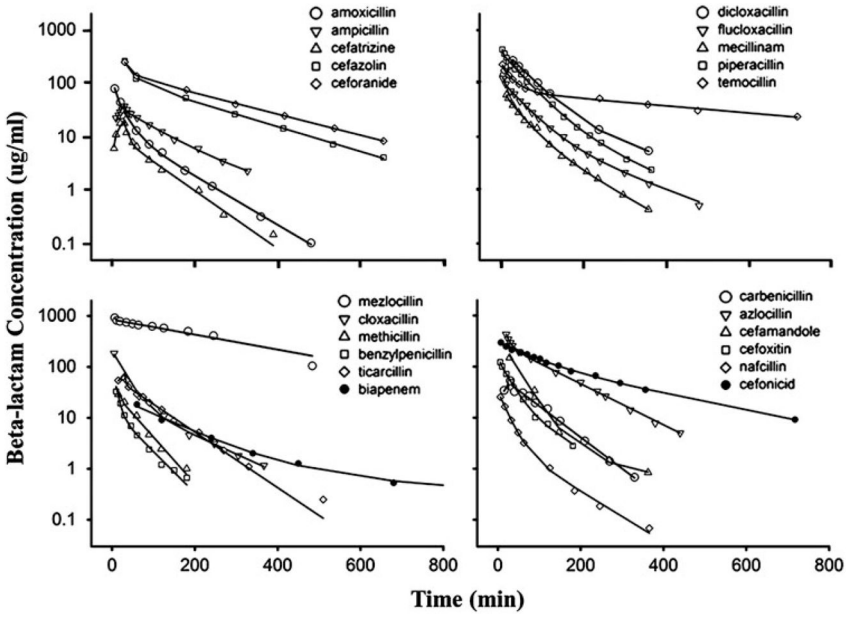

Fig. 5.
Pharmacokinetic profiles of 22 beta-lactams in human subjects

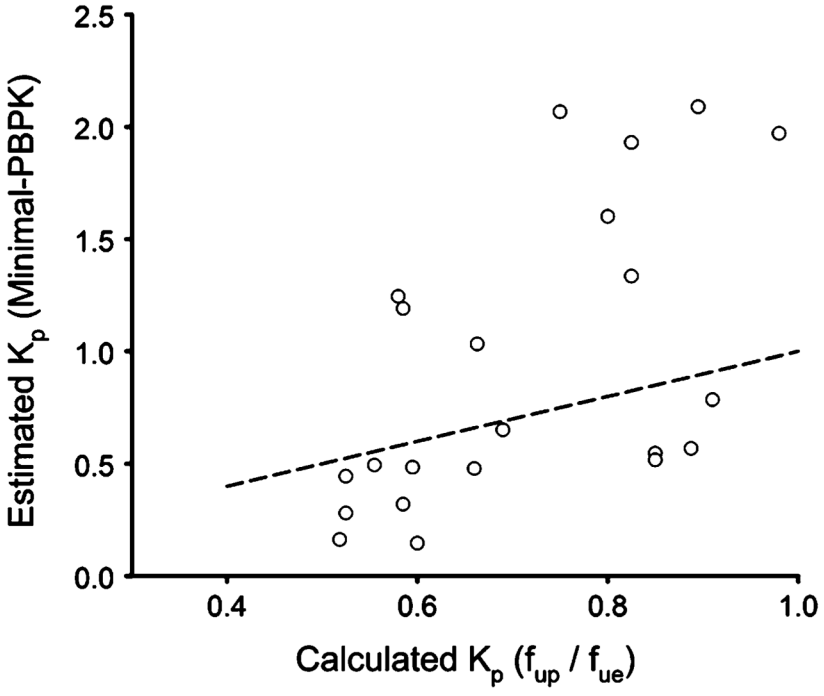

Fig. 6.
Correlation between estimated (K_p) and calculated partition coefficients K_p (f_{up}/f_{ue}) for 22 beta-lactam antibiotics. The *line* of identity is shown

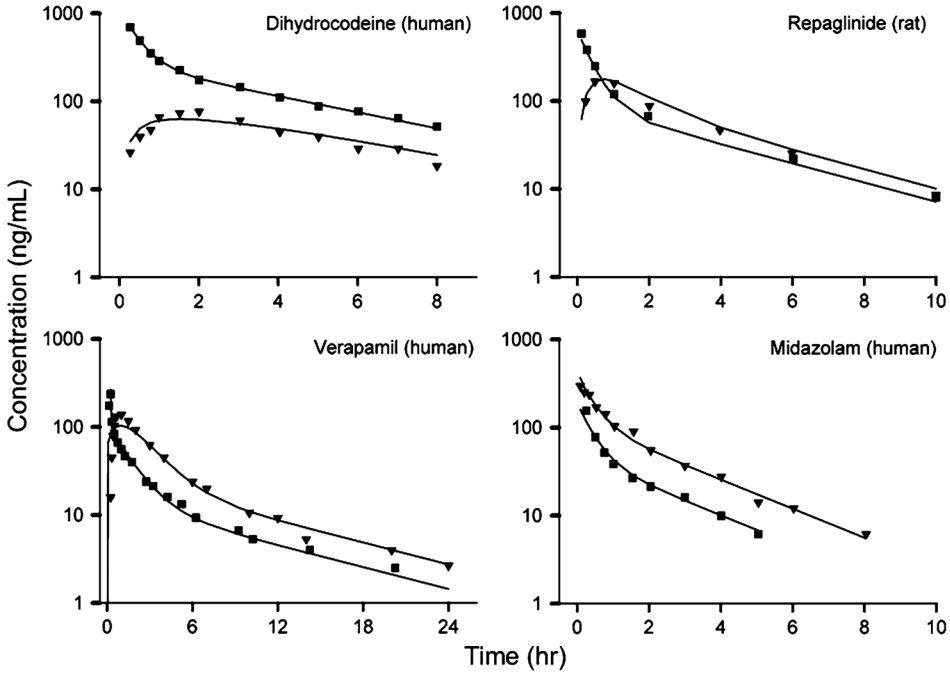

Fig. 7.
Pharmacokinetic profiles for four selected drugs after oral (*triangle*) and IV (*square*) dosing

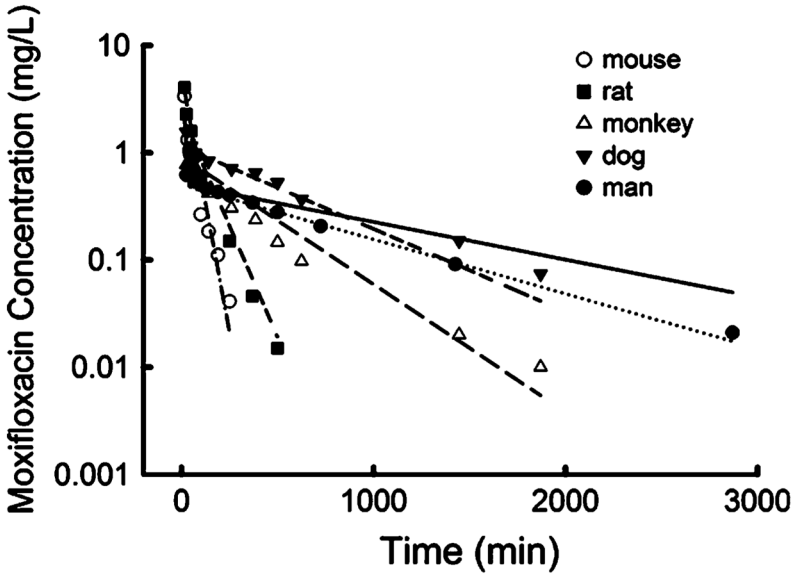

Fig. 8.
Pharmacokinetic profiles for moxifloxacin in five species. The *dotted line* provides fitting with an adjusted *b* value for man

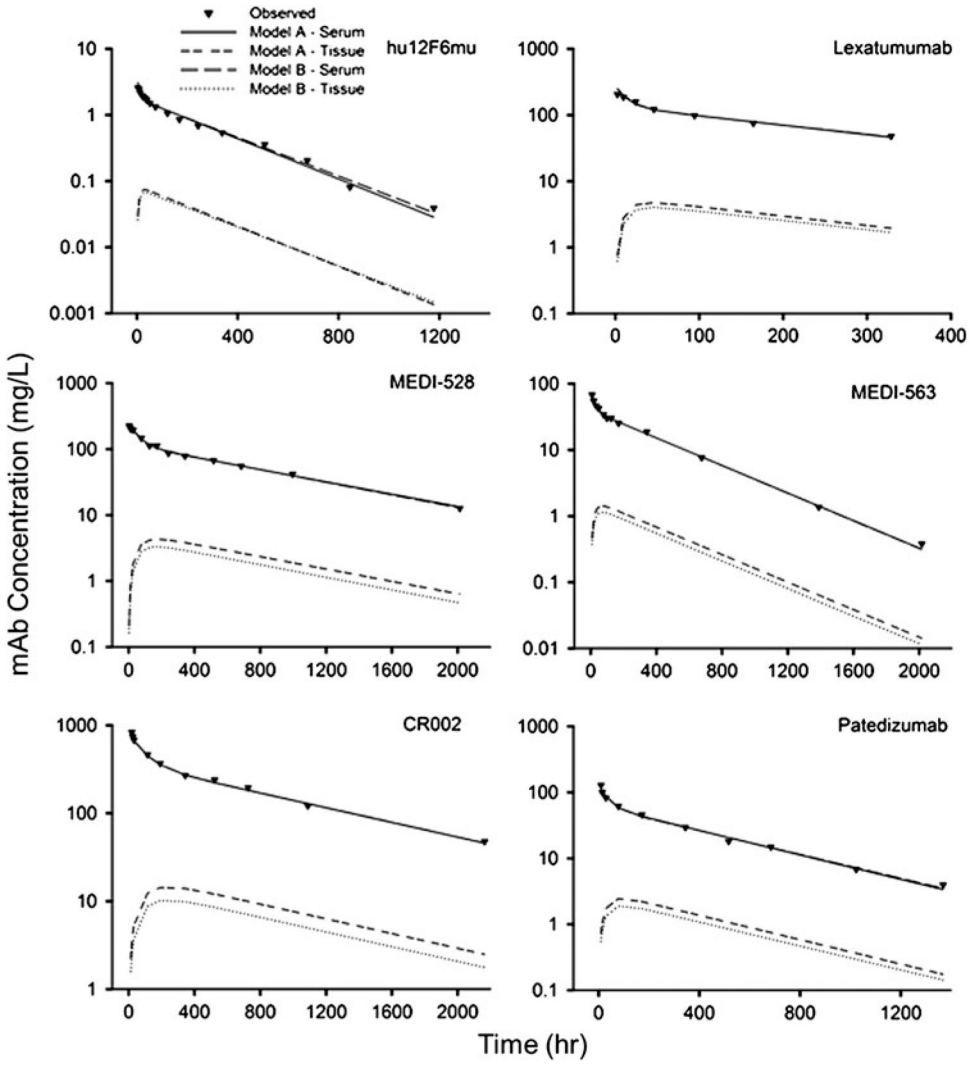

Fig. 9.
Pharmacokinetic profiles for six mAbs given to human subjects and simulated tissue concentrations

Table 1

Final estimated pharmacokinetic parameters (CV %) for 22 beta-lactam antibiotics in human subjects

Drugs [ref]	Dose (mg)	Dosing	Model	f_{up}	K_p	f_{d1}	f_{d2}	V_1 (L)	CL (L/min)	V_{ss} (L)
Amoxicillin [17]	1,000	IV bolus	II[a]	0.82	0.785 (9.25)	0.0180 (26.4)	0.0737 (40.8)	8.26 (14.5)	0.298 (3.73)	15.4 (6.13)
Ampicillin [18]	1,000	INF (30 min)[b]	II	0.79	2.089 (95.08)	0.00674 (45.8)	0.419 (11.8)	4.05 (19.9)	0.235 (16.9)	32.4 (79.8)
Cefatrizine [19]	260	INF (30 min)	I[c]	0.38	0.651 (7.89)	0.0515 (14.5)	–	–	0.231 (2.98)	13.7 (4.88)
Cefazolin [20]	2,000	IV bolus	I	0.11	0.494 (4.69)	0.0229 (10.5)	–	–	0.0747 (1.72)	11.6 (2.59)
Ceforanide [20]	2,100	INF (30 min)	I	0.19	0.484 (2.62)	0.0321 (7.40)	–	–	0.0576 (0.879)	11.5 (1.43)
Dicloxacillin [21]	2,000	INF (30 min)	I	0.04	0.162 (118)	0.00208 (34.0)	–	–	0.0812 (7.57)	7.30 (34.0)
Flucloxacillin [22]	1,000	INF (5 min)	II	0.05	0.445 (10.5)	0.0988 (14.7)	0.00409 (14.6)	6.77 (8.97)	0.141 (1.31)	11.0 (5.53)
Mecillinam [23]	700	INF (15 min)	II	0.78	0.568 (6.21)	0.372 (95.6)	0.00626 (24.2)	8.42 (6.40)	0.200 (2.19)	12.6 (3.65)
Piperacillin [24]	4,000	INF (5 min)	II	0.70	0.547 (4.97)	0.416 (30.7)	0.00311 (18.2)	9.18 (2.83)	0.190 (1.51)	12.3 (2.87)
Temocillin [25]	2,000	IV bolus	II	0.17	1.19 (4.86)	0.0989 (26.4)	0.0325 (9.97)	2.11 (14.9)	0.0396 (3.38)	21.8 (3.77)
Mezlocillin [26]	4,000	INF (5 min)	II	0.65	1.33 (131)	0.895 (29.4)	0.102 (18.8)	12.7 (36.1)	2.49 (18.7)	22.5 (10.1)
Cloxacillin [27]	1,000	INF (5 min)	I	0.05	0.280 (10.8)	0.00798 (18.3)	–	–	0.141 (3.48)	8.84 (4.47)
Methicillin [28]	1,050	INF (15 min)	I	0.65	1.93 (49.9)	1.000 (0.0433)	–	–	0.693 (42.2)	30.3 (41.3)
Benzylpenicillin [29]	600	IV bolus	I	0.32	0.479 (11.4)	0.0351 (18.2)	–	–	0.381 (3.67)	11.4 (6.20)
Ticarcillin [30]	2,000	INF (30 min)	I	0.60	1.60 (6.32)	0.238 (17.6)	–	–	0.391 (3.22)	26.0 (5.06)
Carbenicillin [30]	2,000	INF (30 min)	I	0.50	2.07 (29.3)	1.000 (0.0264)	–	–	0.479 (25.8)	32.1 (24.5)
Azlocillin [32]	4,160	INF (20 min)	II	0.70	0.517 (2.47)	0.0415 (11.8)	0.0755 (37.4)	10.8 (4.66)	0.125 (1.03)	11.9 (1.39)
Cefamandole [33]	2,000	INF (30 min)	I	0.20	0.146 (51.6)	0.00143 (14.9)	–	–	0.149 (4.01)	7.10 (13.8)
Cefonicid [36]	2,100	IV bolus	II	0.18	0.320 (13.9)	0.00306 (20.4)	0.148 (29.2)	7.42 (6.88)	0.0432 (1.26)	9.36 (2.34)
Biapenem [31]	300	INF (30 min)	II	0.96	1.94 (10.7)	0.996 (–)	0.00444 (8.11)	4.72 (7.49)	0.0998 (3.24)	30.4 (8.91)
Cefoxitin [34]	2,100	IV bolus	II	0.33	1.03 (21.6)	0.362 (9.61)	0.0160 (14.5)	7.05 (20.4)	0.390 (3.62)	18.6 (15.6)
Nafcillin [35]	500	IV bolus	II	0.16	1.24 (8.52)	0.979 (0.0529)	0.0203 (0.12)	6.06 (9.00)	0.512 (1.58)	21.4 (6.45)

Assumed 70 kg body weight. All symbols are defined in text

[a] Minimal-PBPK model with two tissue compartments

[b] Intravenous infusion (duration)

[c] Minimal-PBPK model with one tissue compartment

Table 2

Final estimated pharmacokinetic parameters (CV %) for hepatic extraction drugs

Parameter (units)	Definition	Dihydrocodeine	Verapamil	Repaglinide	Midazolam
Species (Body Weight)	/	Man (70 kg)	Man (70 kg)	Rat (250 g)	Man (70 kg)
Oral dose	/	30 mg	120 mg	0.5 mg/kg	10 mg
IV dose	/	30 mg	15 mg (INF, 15 min)[a]	0.2 mg/kg	9.6 mg
f_{d1}	Fraction of Q_{CO} for V_1	0.892 (3.77)	0.903 (1.92)	0.979 (0.00)	0.692 (87.4)
f_{d2}	Fraction of Q_{CO} for V_2	0.108 (NA)	0.097 (NA)	0.021 (NA)	0.0842 (27.3)
K_p	Partition coefficient	0.940 (4.32)	3.96 (12.5)	0.914 (8.74)	0.655 (9.69)
k_a (1/min)	Absorption rate constant	0.00754 (10.3)	0.0150 (12.6)	0.0176 (12.1)	0.218 (154)
CL_{intu} (L/min or mL/min)	Hepatic intrinsic clearance	0.424 (158)	1.34 (59.0)	1.70 (3.48)	0.711 (8.20)
CL_{hep} (L/min or mL/min)	Hepatic clearance	0.328	0.696	1.45	0.477
$CL_{non\text{-}hep}$ (L/min or mL/min)	Non-hepatic clearance	NA	0.214 (28.8)	NA	NA
ER[b]	Hepatic extraction ratio	0.245	0.520	0.148	0.329
V_1 (L or mL)	Tissue compartment 1	46.2 (1.47)	21.3 (13.0)	53.5 (15.2)	24.3 (14.4)
F_G	Pre-hepatic bioavailability	0.409 (6.21)	0.553 (2.75)	0.500 (0.236)	0.742 (12.4)
V_{ss} (L or mL)	Steady-state volume	64.5 (3.97)	346 (11.6)	230 (8.23)	46.5 (8.61)
Bio[c]	Bioavailability based upon NCA	0.266	0.217	0.328	0.453

[a] Intravenous infusion (duration)

[b] ER, calculated according to Eq. (8)

[c] calculated as $(AUC_{oral}/D_{oral})/(AUC_{iv}/D_{iv})$ with AUC from noncompartmental analysis (NCA)

Table 3

Pharmacokinetic parameters of moxifloxacin across five species

Species	Body Wt, kg	Dose mg/kg
Mouse	0.02	9.2
Rat	0.25	9.2
Monkey	5	2.8
Dog	10	2.8
Man	70	1.2

Parameter	Definition	Value	CV%
f_d	Fraction of Q_{CO} for V_1	1.00	< 0.01
K_p	Partition coefficient	2.70	7.57
a	Normalization constant for CL	0.014	5.75
b	Scaling exponent for CL	0.591	2.18
b_{hum}	Scaling exponent for CL in man	0.691	3.07

Table 4

Pharmacokinetic parameters (CV %) for six monoclonal antibodies (mAb) in human subjects

mAb [Ref]	Dose[a]	Model A: *CL* from tissue				Model B: *CL* from plasma			
		f_d (−)	K_p (−)	CL_T (L/h)	AUC_R^b	f_d (−)	K_p (−)	CL_P (L/h)	AUC_R^b
Hu12F6mu [42]	10 mg	0.00111 (15.3)	0.0522 (8.86)	0.412 (9.18)	0.045	0.000936 (18.1)	0.0429 (6.61)	0.0187 (2.83)	0.042
Lexatumumab [43]	10 mg/kg	0.000692 (25.0)	0.0475 (19.9)	0.404 (24.6)	0.037	0.000562 (26.8)	0.0346 (15.2)	0.0162 (7.62)	0.032
MEDI-528 [44]	9 mg/kg	0.000156 (10.9)	0.0562 (9.62)	0.126 (9.48)	0.042	0.000123 (13.5)	0.0330 (5.17)	0.00553 (1.79)	0.031
MEDI-563 [45]	3 mg/kg	0.000398 (7.69)	0.0519 (5.30)	0.289 (3.80)	0.041	0.000320 (9.56)	0.0337 (3.56)	0.0121 (1.45)	0.033
CR002 [46]	30 mg/kg	0.000110 (31.2)	0.0664 (29.8)	0.106 (23.1)	0.046	0.0000779 (43.6)	0.0333 (20.7)	0.005 (6.58)	0.031
Pateclizumab [47]	5 mg/kg	0.000310 (14.5)	0.0607 (12.6)	0.241 (9.58)	0.045	0.000231 (19.7)	0.0368 (8.82)	0.0112 (2.63)	0.035

[a] Assumed 70 kg body weight

[b] AUC_{tissue}: AUC_{serum} ratio